Received: 21 November 2022 | Revised: 8 February 2023 | Accepted: 7 March 2023

DOI: 10.1002/jsp2.1254

RESEARCH ARTICLE

JOR Spine OPEN ACCESS

Galectin-3 and RAGE differentially control advanced glycation endproduct-induced collagen damage in murine intervertebral disc organ culture

Zachary S. Gallate | Danielle N. D'Erminio | Philip Nasser | Damien M. Laudier | James C. Iatridis

Leni & Peter W. May Department of Orthopedics, Icahn School of Medicine at Mount Sinai, New York, New York, USA

Correspondence
James C. Iatridis, Leni & Peter W. May Department of Orthopaedics, Icahn School of Medicine at Mount Sinai, 1 Gustave Levy Place, Box 1188, New York, NY 10029-6574, USA.
Email: james.iatridis@mssm.edu

Funding information
National Institute of Arthritis and Musculoskeletal and Skin Diseases, Grant/Award Numbers: R01AR069315, R01AR078857, R01AR080096; NIAMS

Abstract

Background: Back and neck pain are leading causes of global disability that are associated with intervertebral disc (IVD) degeneration. Causes of IVD degeneration are multifactorial, and diet, age, and diabetes have all been linked to IVD degeneration. Advanced glycation endproducts (AGEs) accumulate in the IVD as a result of aging, diet, and diabetes, and AGE accumulation in the IVD has been shown to induce oxidative stress and catabolic activity that result in collagen damage. An association between AGE accumulation and IVD degeneration is emerging, yet mechanism behind this association remains unclear. The Receptor for AGEs (RAGE) is thought to induce catabolic responses in the IVD, and the AGE receptor Galectin 3 (Gal3) had a protective effect in other tissue systems but has not been evaluated in the IVD.

Methods: This study used an IVD organ culture model with genetically modified mice to analyze the roles of RAGE and Gal3 in an AGE challenge.

Results: Gal3 was protective against an AGE challenge in the murine IVD ex vivo, limiting collagen damage and biomechanical property changes. Gal3 receptor levels in the AF significantly decreased upon an AGE challenge. RAGE was necessary for AGE-induced collagen damage in the IVD, and RAGE receptor levels in the AF significantly increased upon AGE challenge.

Discussion: These findings suggest both RAGE and Gal3 are important in the IVD response to AGEs and highlight Gal3 as an important receptor with protective effects on collagen damage. This research improves understanding the mechanisms of AGE-induced IVD degeneration and suggests Gal3 receptor modulation as a potential target for preventative and therapeutic treatment for IVD degeneration.

KEYWORDS
advanced glycation endproducts, collagen damage, degeneration, Galectin-3, intervertebral disc, receptor for advanced glycation endproducts (RAGE)

Zachary S. Gallate and Danielle N. D'Erminio contributed equally.

1 | INTRODUCTION

Back and neck pain is a leading cause of global disability and is associated with an economic burden ranging from $12 billion to $90 billion in the United States [1]; and chronic pain significantly increases risks of depression, anxiety, and sleep disorders [2]. Intervertebral disc (IVD) degeneration is highly associated with back pain, and is increased with aging [3]. Fissuring or other damage to the annulus fibrosus (AF) is common in IVD degeneration and can be a direct source of pain or chronic proinflammatory conditions [4–6]. The AF is largely composed of long-lived extracellular matrix proteins, especially collagens. Collagen type I is most abundant in the outermost periphery of the AF and collagen type II is most abundant in the inner AF and Nucleus Pulposus (NP) regions [7].

High-AGE diets and diabetes was demonstrated in animal models to result in advanced glycation endproduct (AGE) accumulation in the IVD, with associated IVD degeneration, collagen damage, and altered biomechanical properties [8–15]. Collagens and other long-lived matrix proteins in the AF are susceptible to mechanical damage as well as proteolytic degradation due to oxidative and pro-inflammatory environments [16]. Collagens accumulate AGEs during aging, that can increase oxidative stress and accelerate matrix metalloproteinase activity [9]. Poor diet and diabetic conditions can accelerate AGE accumulation, resulting in accelerated IVD degeneration in vivo in mice [8,17–19]. Fields et al. showed an association between AGE accumulation in diabetic rats, increased oxidative stress, and IVD stiffness [8]. AGEs bind to collagens forming AGE adducts [20], that were linked to increased TNF-α activity and catabolism [18]. Additionally, AGEs can form crosslinks between collagen proteins, which causes a stiffer and more brittle matrix [10,12]. Improved understanding of the mechanisms whereby AGE accumulation results in AF collagen damage may inform future therapeutic strategies.

AGEs interact with two main receptors for AGEs: the AGE Receptor Complex, and the Receptor for AGEs (RAGE) [21] (Figure 1). RAGE is a cell surface receptor, though a splicing variant of RAGE known as soluble RAGE (sRAGE) is secreted extracellularly [21]. Binding through RAGE is known to be pro-catabolic and has therefore received the most research focus in IVD studies [13,18,23]. Systematic ablation of RAGE in mice, $RAGE^{-/-}$, referred to as RAGE knockout (RAGE-KO), was protective of AGE-induced collagen damage and altered biomechanical properties [13,24]. The AGE-Receptor Complex, made up of OST-48 (AGE-R1), 80K-H (AGE-R2), and Galectin 3 (Gal3), (AGE-R3), can interact with and bind to AGEs through Gal3 [21] (Figure 1). Gal3 is a member of the lectin family and has a high binding affinity of AGE ligands [25]. Gal3 does not have a transmembrane domain, but interacts with OST-48, and 80K-H [21,26,27] to play a role in cell signaling. Gal3 has been shown to be protective of AGE-induced damage in other tissues, including in adipose tissue, pancreatic islets, and the kidneys [28–32]. The role of Gal3 in the IVD as an AGE receptor is mostly unknown; however, it has been studied in the IVD in relation to its role in the hypoxic response [33]. In IVD cell culture, Gal3 has been suggested to play a role in modulating NF-KB and TGF-β signaling, and to influence catabolic and pro-inflammatory responses following TNF-α challenge [34,35]. Gal3 therefore appears to play a context dependent role which at times can be protective against AGE challenge. Determining the roles of AGE receptors to stressors in the IVD is important to inform healthy lifestyle and identify potential therapeutic targets that promote IVD health and prevent its degeneration. No studies on the IVD have investigated RAGE and Gal3 together.

This study determined the relative contributions of RAGE and Gal3 to an AGE challenge in a mouse IVD organ culture experiment. We hypothesized that Gal3 and RAGE differentially affect the IVD response to an AGE challenge. We utilized genetically modified mice that ablate, or knockout, Gal3 (Gal3-KO) and RAGE (RAGE-KO) to inhibit Gal3 and RAGE signaling processes, respectively, and C57Bl6 wildtype controls. Coccygeal IVDs were used in a whole IVD ex vivo organ culture model to investigate the roles of RAGE and Gal3 in response to an AGE challenge. Organ culture was used because it is a highly controlled model system that can focus on the responses of IVD cells and tissues without influence of systemic effects. Effects of AGEs on IVDs were assessed using multiple output measurements including collagen damage, IVD degeneration grading, and functional biomechanical testing. Immunohistochemical (IHC) assays for Gal3 and RAGE confirmed genetic ablation, and were used to evaluate the changes of receptor levels in response to an AGE challenge. Collagen

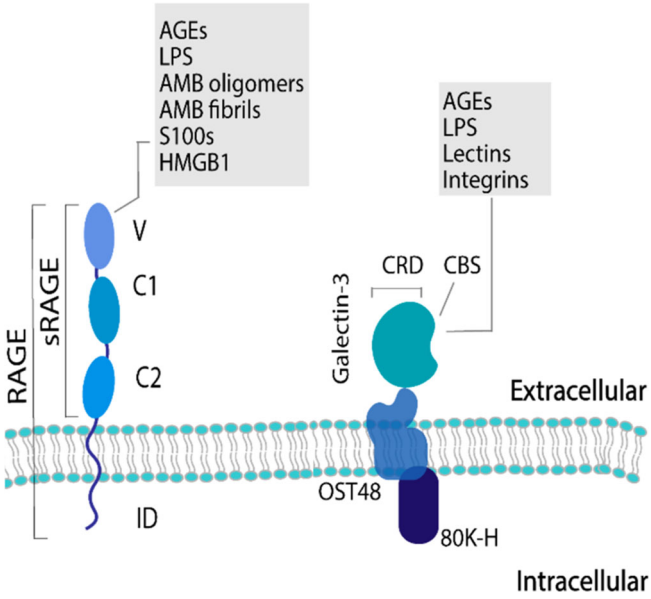

FIGURE 1 Structure and ligands for RAGE and Gal3. Structure and ligands of the receptor for advanced glycation end products (RAGE) and soluble form of RAGE (sRAGE), and AGE receptor complex including galectin-3 (Gal3). The ligand-binding domains of the different receptors are: V-domain (V), C1- and C2-domain (C1 and C2), and intracellular-domain (ID), oligosaccharyltransferase 48 complex (OST48), 80K-H, carbohydrate-binding site (CBS), and carbohydrate recognition domain (CRD). The ligands for the different receptors are advanced glycation end products (AGEs), lipopolysaccharide (LPS), amyloid-β (AMB), S100s, high mobility group protein 1 (HMGB1), lectins, and integrins. Figure adapted with permission from Noriega et al. [22].

damage and immunostaining focused on the AF region because the abundance of collagen in that region made it most sensitive to AGE-induced collagen damage.

2 | MATERIALS AND METHODS

2.1 | Ex vivo organ culture and study design

An ex vivo organ culture model exposed male RAGE-KO, Gal3-KO, and wildtype murine IVDs to an AGE challenge (Figure 2). Gal3-KO mice were purchased from The Jackson Laboratory (Strain #006338) ($n = 8$). The original RAGE-KO mouse lineage was donated from the Ann Marie Schmidt laboratory, and the mice used in this study were bred and maintained at Mount Sinai ($n = 8$). C57BL/6 mice were used as WT control animals ($n = 9$) as both the Gal3-KO and RAGE-KO mice were bred on a C57Bl/6 background. At 4–5 months of age, 6 caudal mouse IVDs were isolated from each mouse including coccygeal (c) c3/4, c4/5, c6/7, c8/9, c10/11, and c11/12 levels with a portion of the superior and inferior vertebrae attached yielding vertebral motion segments. No live animals were used for this study, although breeding was involved. All studies were performed with IACUC approval.

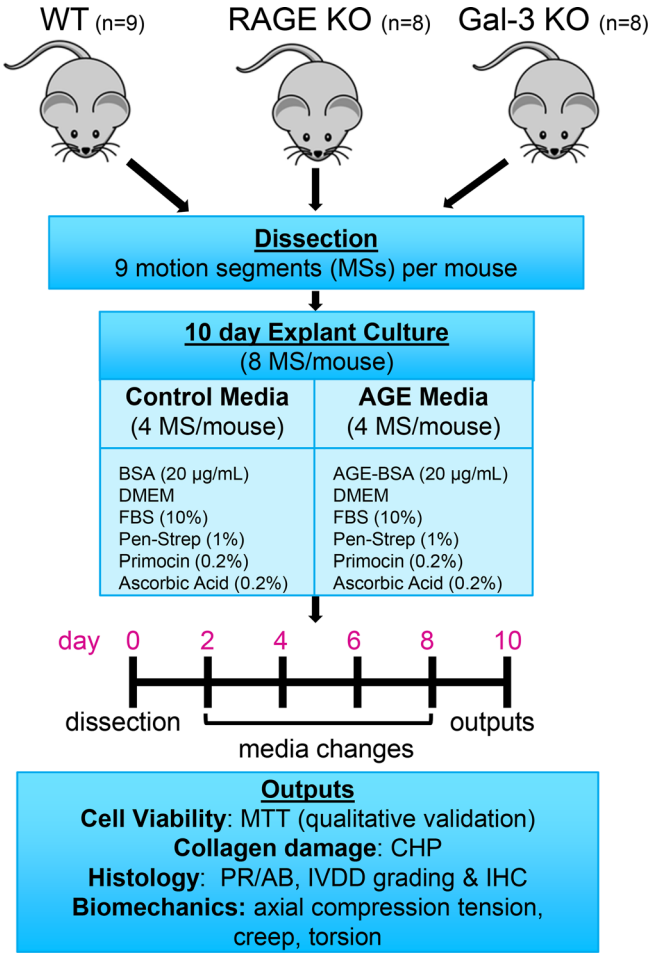

FIGURE 2 Study design. Three separate groups of genetically altered murine with dissections of caudal motion segments from male wildtype ($n = 9$), RAGE-KO ($n = 8$), and Gal3-KO ($n = 8$) mice. After 10 days, three paired motion segments (MSs) from each mouse were used for cell viability, collagen damage and histology, and biomechanics measurements. Culture conditions were 37°C, 5% O_2, 5% CO_2, 90% N_2, and >90% humidity, with gentle rocking and media changes every 2 days.

Organ culture conditions were 37°C, 5% O_2, 5% CO_2, 90% N_2, and >90% humidity with gentle rocking + media change every 2 days, as described previously [13]. Mouse IVDs from the c3/4 and c4/5 level were used for histological analysis to determine levels of collagen damage [36], IVD degeneration [37,40], and receptor abundance. Mouse IVDs from the c6/7 and c8/9 levels were used for biomechanical testing to determine the biomechanical functional changes resulting from an AGE challenge and the role of AGE receptors in these changes. Mouse IVDs from the c10/11 and c11/12 levels were used to assess cell viability. Control media contained Dulbecco's Modified Eagle's Medium (DMEM), 10% fetal bovine serum (FBS), 1% Pen-Strep, 0.2% Primocin, 0.2% Ascorbic Acid, and 20 µg/mL bovine serum albumin (BSA). Experimental AGE media (+AGEs) was identical with the control media except for the replacement of 20 µg/mL BSA with 20 µg/mL AGE-BSA (ab51995; Abcam).

2.2 | Cell viability, collagen damage, degeneration grading, and Immunohistochemistry

Following organ culture, IVDs designated for histological and immunohistochemical analyses were fixed in zinc formalin (Z-Fix, Anatech LTD, Battle Creek, MI, USA) for at least 48 h. Samples were then processed and embedded in methyl-methacrylate (MMA, m55909, Sigma–Aldrich) to best retain IVD structure [38,39]. Serial sagittal sections (5 µm thick) were taken from each sample using a sledge microtome (Leica SM2500 base). All microscopic imaging was performed on a Leica DM 6B widefield microscope at 20× magnification. For quantitative analyses, exposure times and bulb intensities were kept consistent for all compared samples. For quantification of AF regions, we selected regions of interest (ROI) to include the outermost 5 ± 2 lamellar layers of the AF. The outer AF was prioritized for quantification as the regions demonstrating the clearest effects and the layers that were most affected by AGE diffusion into the IVD.

IVD organs designated for cell viability were incubated with thiazolyl blue tetrazolium bromide (MTT, Sigma–Aldrich, St. Louis, MO), which stains viable cells, using 1 mg/mL MTT in culture media overnight prior to the completion of culturing. Samples were then fixed in Z-Fix, embedded in MMA, sectioned, and stained with 4′,6-diamidino-2-pheylindole (DAPI, Roche Diagnostics, Germany). The presence of distinct MTT staining in close proximity to DAPI confirmed cellular activity of viable cells as described previously [41].

To investigate the extent and localization of collagen damage within each IVD, samples were stained with Collagen hybridizing peptide (CHP) as described [12,36,42,43]. CHP is a small synthetic peptide with glycine-proline-hydroxyproline repeats that can hybridize with unfolded collagen α chains, and therefore CHP binding can

be used to detect and image molecular level subfailure collagen damage in multiple collagenous tissues [12,13,36,42,43,44]. CHP was conjugated with biotin (B-CHP; BIO300, 3Helix Inc; Salt Lake City, UT). Positively bound CHP was detected using streptavidin labeled with WARP Red (Biocare Medical, Concord, CA) fluorescing chromogen. Murine IVDs designated as positive control samples were dissected, stored at −80°C, thawed, and placed in histology cassettes in a glass beaker with distilled water and subjected to 90°C for 180 min to induce collagen protein damage throughout the IVD. Warp Red staining without counterstain was quantified by analyzing the sample staining intensity and applying background subtraction with an upper pixel intensity threshold to include stained pixels and exclude pixels in the ROI without tissue present. Toluidine blue counterstain better displayed AF anatomy, yet was not used for quantification of collagen damage in this study since it impacted WARP Red quantification even when using color deconvolution algorithms. Pixel intensity was measured using ImageJ software to calculate the amount of collagen damage in samples as described previously [13,36,42]. Inverse pixel intensity values were used when measuring samples under bright-field light to accurately reflect light absorption rather than light emission.

IVD degeneration in murine IVD tissues was quantified using the Rutges degeneration grading scheme [37], with consideration for murine IVD morphology [40]. Three independent and blinded spine researchers graded IVDs for degeneration as recommended [37,40].

IHC was used to analyze the levels of Gal3 and RAGE receptor levels using anti-rabbit Gal3 primary antibody and anti-rabbit RAGE primary antibody (abcam, Waltham, MA). IHC protocols included deplasticization with xylene for 30 min and EGME for 5 min, histozyme for 6 min to retrieve epitopes hidden or damaged during embedding or storage, and 2.5% normal horse serum for 20 min to block non-specific antibody binding. The Gal3 primary antibody solution was made in 1:200 µL ratio of Gal3 antibody to diluent, and samples were incubated for 1 h. For Gal3, the secondary antibody was horse anti-rabbit IgG alkaline phosphatase (Vector Laboratories, San Francisco, CA) for 30 min with WARP Red (Biocare Medical, Concord, CA) fluorescing chromogen for 10 min and DAPI to localize cell nuclei. RAGE primary antibody solution (1:400 µL) for 1 h, with Amplifier Antibody for 15 min and polymer reagent for 30 min (Vector Laboratories, San Francisco, CA), followed by ImmPACT 3, 3′-diaminobenzidine (DAB) solution for 6 min, and Toluidine Blue counterstaining. For Gal3 and RAGE, murine lung tissue was used as a positive tissue control, as RAGE is highly expressed in lung [45]. Negative control samples were treated with non-immune rabbit serum instead of the primary.

Cell counting was used to quantify changes in the levels of Gal3 in the IVD after an AGE challenge. The mean pixel intensity of the ROI of the technical negative sample of each biological replicate was used as a lower threshold, and intensity values within cells above this threshold were considered positive staining for all samples from that biological replicate. Cells within the ROI were then counted manually by DAPI-positive staining and morphology to attain the total cell count within the ROI. Gal3 positive and RAGE positive cells were then counted to obtain a percent positive cell count within each sample for each receptor.

2.3 | Biomechanical analyses

Axial tension and compression, creep tests, and torsional tests were conducted on c6/7 and c8/9 murine IVD motion segments of all genotypes as described [46,47]. Axial compression-tension and creep testing were conducted on an ElectroForce 3200 (TA Instruments, New Castle, DE) and torsional testing was conducted on a AR2000x Rheometer (TA Instruments, New Castle, DE). Vertebrae were fixed in stainless steel cylindrical pots with cyanoacrylate and then hydrated in PBS. Motion segments were first subjected to 20 cycles of axial tension and compression at ±0.5 N, 1 Hz followed by 45 min of compressive creep testing at 0.5 N. Motion segments were then rehydrated in PBS for 45 min before undergoing torsional testing consisting of 20 cycles of ±20° torsional rotation at 1 Hz. All measurements conducted after cyclical force application were recorded on the 20th cycle of force application using MATLAB. Biomechanical parameters including neutral zone length, stiffness, and creep elastic response (Se), fast and slow response time constants (t1 and t2 respectively) and fast and slow stiffness parameters (S1 and S2 respectively) were calculated using Matlab.

2.4 | Statistical analyses

Bar graphs were created in GraphPad Prism v9 (GraphPad, La Jolla, CA); each data point represents one biological replicate, bars indicate group mean, and error bars indicate one standard deviation. Correlation analyses were created in Rstudio, in which each data point represents a single murine IVD.

All data was analyzed in Rstudio (Boston, MA). The Shapiro–Wilk test confirmed normality of the data. Statistical differences were determined using repeated measures ANOVA to determine the effect of treatment within biological replicates for collagen damage, degeneration grade, Gal3 and RAGE immunopositivity, and biomechanical properties. The statistical tests focused on detecting the effects of AGE treatment for each genotype since global deletions can impact baseline values of parameters from effects during development and growth that are unrelated to the media interventions applied in this study. All tests applied a significance threshold of $p \leq 0.05$.

3 | RESULTS

3.1 | Cell viability

The 10-day organ culture experiment was successfully performed with extensive MTT staining that was specific and robust indicating nearly all cells were metabolically active and viable (Figure S1). Many cells exhibited clustered staining that did not enable distinction

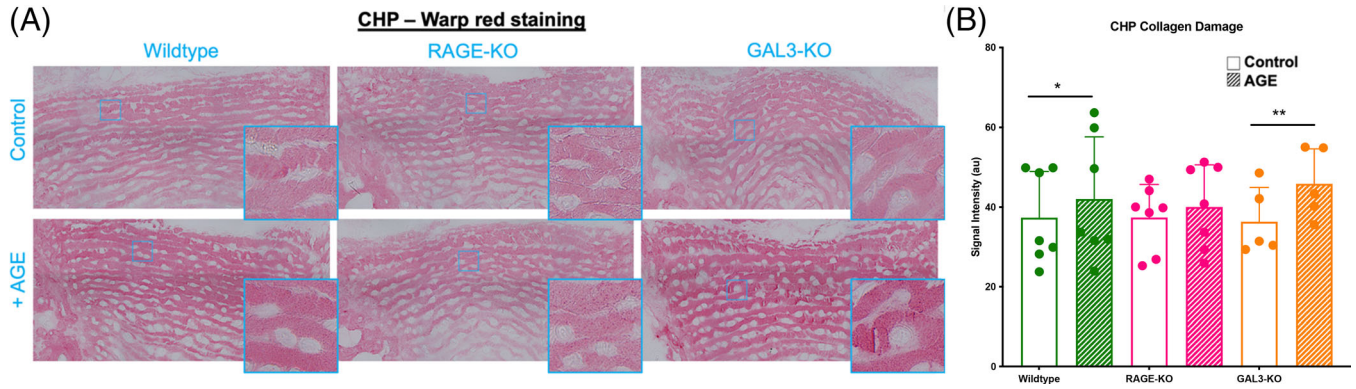

FIGURE 3 AGE challenge increased collagen damage in wildtype and Gal3-KO AF. (A) Murine IVD AFs stained with a CHP primary, and WARP Red chromogen (red) imaged at 20× magnification. Wildtype (left column), RAGE-KO (central column), and Gal3-KO (right column) mice after 10 day culture in control media (top row) or AGE media (bottom row). Increased staining intensity can be seen visually in the wildtype and Gal3-KO murine IVDs that were exposed to AGE media compared to its control media biological replicate. Boxes indicate magnified view and are approximately 50 μm in width. (B) Bar graphs denoting arbitrary units (au) of mean pixel intensities of Murine IVD AFs within the outer lamellar layers ROI. Wildtype (green), RAGE-KO (pink), and Gal3-KO (orange) murine IVD AF after explant culture in control media (clear box) or AGE media (hash box). Each point represents an individual mouse IVD, error bars show one standard deviation. Significant increases in collagen damage denoted by black bars (*$p \leq 0.05$, **$p \leq 0.01$).

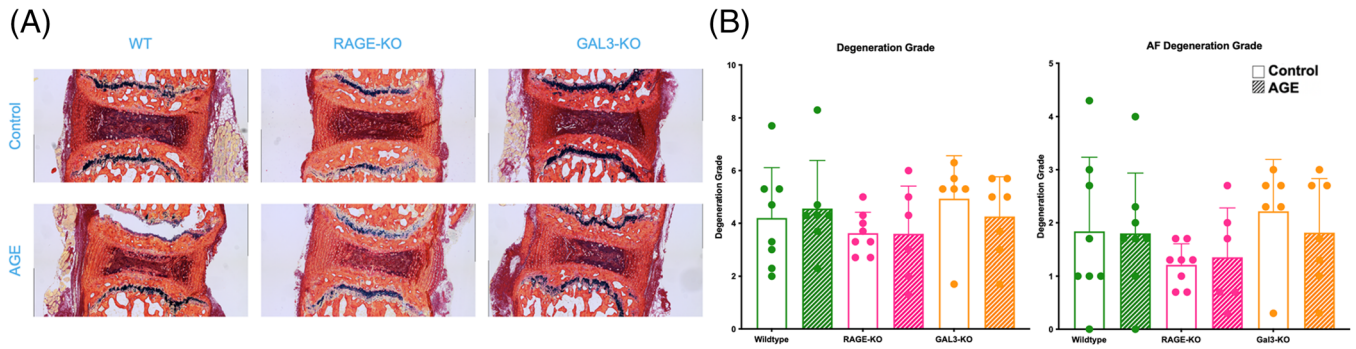

FIGURE 4 AGE challenge did not affect IVD degeneration grade. (A) Murine IVDs stained with picrosirius red (red) and alcian blue (blue), imaged at 20× magnification. Wildtype (left column), RAGE-KO (central column), and Gal3-KO (right column) mice after 10 day culture in control media (top row) or AGE media (bottom row). No significant changes in degeneration as measured by Rutges Grading can be seen upon AGE challenge. (B) Bar graphs denoting Rutges degeneration grade of whole Murine IVDs (left) and exclusively AFs (right). Wildtype (green), RAGE-KO (pink), and Gal3-KO (orange), murine IVD AF after explant culture in control media (clear box) or AGE media (hash box). Each point represents an individual mouse IVD, error bars show one standard deviation. No significant differences between genotype or media can be seen ($p > 0.05$).

between individual DAPI stained cells; therefore, we could not accurately calculate percentage viable cells. The very few cells stained with DAPI alone were located near the cut edge of the outer endplate regions as expected from this organ culture model system.

3.2 | Collagen damage

Collagen damage was increased from AGE challenge in wildtype and Gal3-KO mice, but not in RAGE-KO mice. AF regions of all IVDs were stained broadly for WARP Red, which indicates widespread baseline levels of collagen damage, which is to be expected from collagen turnover (Figure 3A). In wildtype mice, the AGE challenge resulted in a deep red staining indicating increased collagen damage which is supported by significant increases in collagen damage when quantified by CHP ($p \leq 0.039$, Figure 3B). AGE challenge also increased WARP Red staining in Gal3-KO mice ($p \leq 0.002$), but had no effect in RAGE-KO ($p = 0.35$, Figure 3B).

3.3 | Degeneration analysis

IVD degeneration grade was not altered with AGE challenge for any groups in this 10 day organ culture experiment ($p > 0.05$ for all, Figure 4).

3.4 | Immunohistochemical analyses

AGE challenge increased Gal3 receptor staining in wildtype mice shown by a greater percentage of Gal3-positive cells ($p \leq 0.021$;

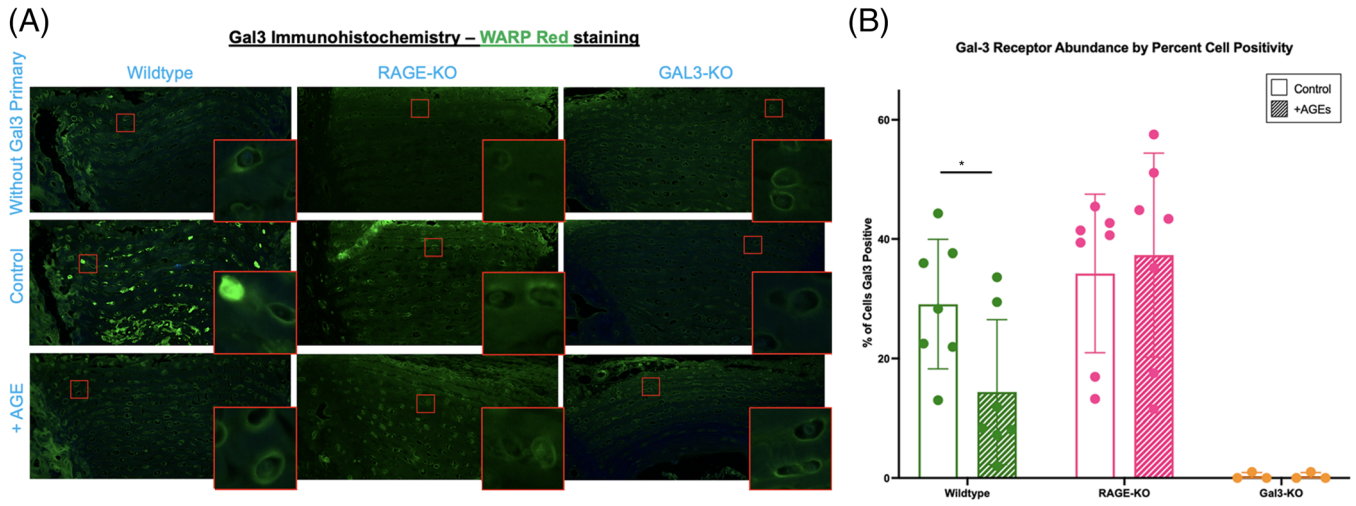

FIGURE 5 AGE challenge reduced Gal3 levels in Wildtype but not RAGE-KO AF. (A) Murine IVD AF stained with a Gal3 primary antibody and WARP Red fluorescing chromogen (green) imaged at 20× magnification. Wildtype (left column), RAGE-KO (central column), and Gal3-KO (right column) mice after 10 day organ culture in control media (middle row) or AGE media (bottom row). Top row shows samples stained without the Gal3 primary indicating fluorescence levels above which are considered positive staining. Cells positively staining for Gal3 can be seen in green. Upon AGE challenge, a decrease in percent cell positivity can be seen visually in the Wildtype murine IVD compared to its control media biological replicate. Gal3-KO murine IVDs do not show cell staining above the threshold set by the technical negative samples. Boxes indicate areas of increased magnification and are approximately 50 µm wide. (B) Bar graphs denoting percent cell positivity of Murine IVD Afs within the outer lamellar layer ROI. Wildtype (green), RAGE-KO (pink), and Gal3-KO (orange) murine IVD AF after explant culture in control media (clear box) or AGE media (hash box). Each point represents an individual mouse IVD, error bars show one standard deviation. Significant decreases in Gal3 percent cell positivity denoted by black bars (*$p \leq 0.01$).

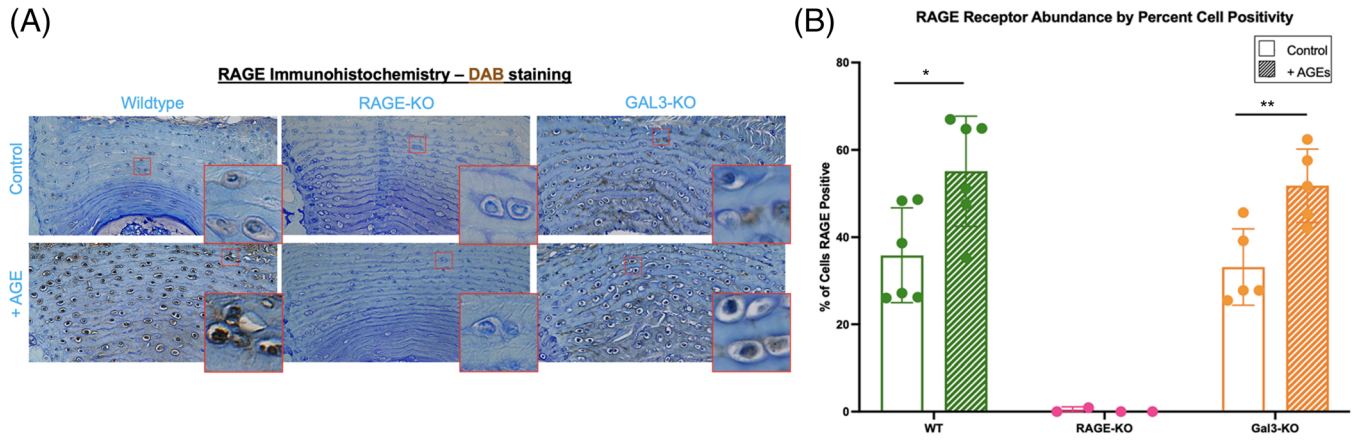

FIGURE 6 AGE challenge increased RAGE in Gal3-KO and Wildtype AF. (A) Immunohistochemistry of murine IVDs using an anti-RAGE primary and DAB (brown) counterstained with toluidine blue (blue) imaged at 20× magnification. Wildtype (left column), RAGE-KO (central column), and Gal3-KO (right column) mice after 10 day culture in control media (top row) or AGE media (bottom row). Cells positively staining for RAGE can be seen in brown. Upon AGE challenge, an increase in percent cell positivity can be seen visually in the Wildtype and Gal3-KO murine IVD compared to their control media biological replicates. RAGE-KO murine IVDs do not show RAGE positive cell staining. Boxes indicate areas of increased magnification and are approximately 50 µm in width. (B) Bar graphs denoting percent cell positivity of Murine IVD Afs within the outer lamellar layer ROI. Wildtype (green), RAGE-KO (pink), and Gal3-KO (orange) murine IVD AF after explant culture in control media (clear box) or AGE media (hash box). Each point represents an individual mouse IVD, error bars show one standard deviation. Significant increases in RAGE percent cell positivity denoted by black bars (*$p \leq 0.05$, **$p \leq 0.01$).

Figure 5). Gal3-positive cell percentages were not increased in RAGE-KO mice IVDs following AGE challenge ($p = 0.62$). Gal3-KO murine IVDs exhibited negligible staining beyond background autofluorescence, consistent with successful ablation of Gal3 expression in the Gal3-KO mice.

AGE challenge increased RAGE IHC staining in wildtype and Gal3-KO mice ($p \leq 0.008$ and $p \leq 0.026$, respectively; Figure 6). RAGE-KO murine IVDs exhibited comparable staining with the negative control mouse lung tissue indicating success of the receptor knockout (Figure 6).

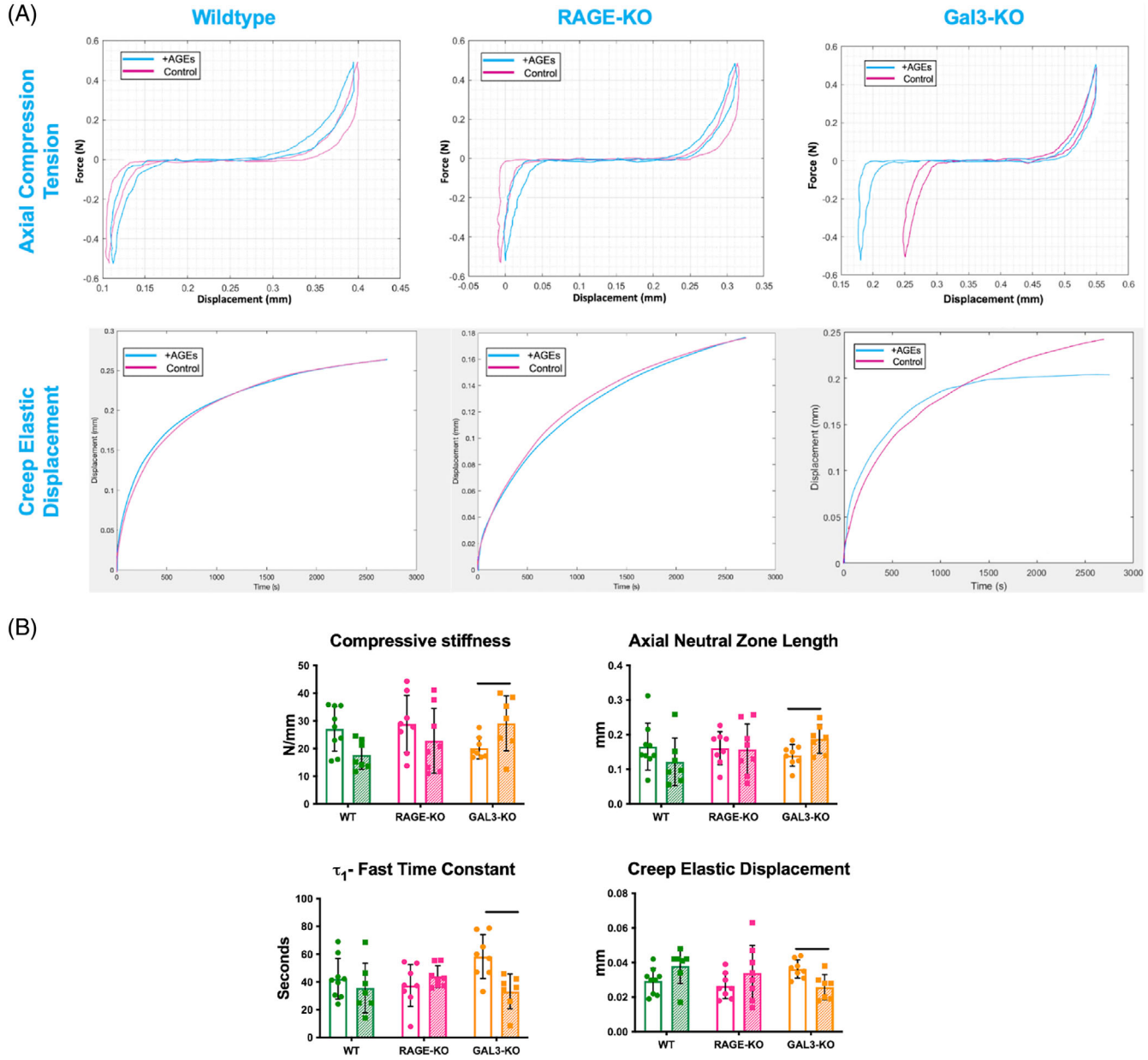

FIGURE 7 AGE challenge altered biomechanical properties of Gal3-KO murine IVDs. (A) Representative axial compression tension curves (top row) and creep elastic displacement (bottom row) for wildtype, RAGE-KO and Gal3-KO murine IVDs. (B) Bar graphs denoting biomechanical properties of murine IVDs with and without AGE challenge. Bars indicate group means. Wildtype (green), RAGE-KO (pink), and Gal3-KO (orange), murine IVD AF after explant culture in control media (clear box) or AGE media (hash box). Each point represents an individual mouse IVD, error bars show one standard deviation. Gal3-KO mouse IVD motion segments have significantly increased compressive stiffness upon AGE challenge ($p \leq 0.034$). Gal3-KO mouse IVD motion segments have significantly increased axial neutral zone lengths upon AGE challenge ($p \leq 0.046$). Gal3-KO mouse IVDs have significantly decreased fast time constants upon AGE challenge ($p \leq 0.024$ Gal3-KO mouse IVDs have significantly decreased Creep Elastic Displacement upon AGE challenge ($p \leq 0.018$).

3.5 | Biomechanical analyses

Biomechanical properties were affected by AGE challenge in Gal3-KO motion segments but not in other genotypes. Specifically, Gal3-KO murine IVDs exposed to AGEs exhibited increased compressive stiffness and increased axial neutral zone length from the axial compression-tension test ($p \leq 0.034$ and $p \leq 0.045$, respectively; Figure 7), suggesting increased laxity with a steeper slope of the load-deflection curve under compressive load possibly due to tissue compaction of bone-to-bone contact. The creep test further determined that AGE challenge in Gal3-KO mice caused decreased creep displacement (consistent with increased compressive stiffness), and a decreased tau1 fast time constant indicating more rapid viscoelastic response ($p \leq 0.018$ and $p \leq 0.024$, respectively; Figure 7). Together, biomechanical results suggest compaction of Gal3-KO mice under AGE challenge that are consistent with collagen damage observed (Figure 3).

4 | DISCUSSION

This study investigated whether AGEs directly affect IVD tissues and cells, and determined relative contributions of the AGE receptors RAGE and Gal3 using an AGE challenge on an IVD organ culture model using Gal3-KO, RAGE-KO and wildtype mice. The most important finding of this study was that Gal3 can play a protective role on IVD structure and functions, since AGE challenge in Gal3-KO IVDs resulted in increased collagen damage, increased RAGE expression, and altered IVD biomechanical properties. AGE challenge in wildtype IVDs increased collagen damage and RAGE immunostaining and decreased Gal3 immunostaining, yet did not result in functional biomechanical alterations indicating the AGE challenge had less severe changes in wildtype than Gal3-KO IVDs. Lastly, AGE challenge did not significantly increase collagen damage or affect biomechanical properties in RAGE-KO IVDs, indicating it plays a role in collagen damage. We therefore conclude that Gal3 is protective and RAGE is destructive in IVD cells and tissues in response to an AGE challenge.

An AGE challenge resulted in collagen damage in WT and Gal3-KO IVDSs, but did not lead to observable morphological IVD degeneration in either of these groups, indicating this is an early and relatively mild challenge. Our study applied highly sensitive CHP assay, which suggests this assay is capable of detecting molecular collagen micro-damage before degeneration is more clearly observable with other histomorphological grading schemes. Zitnay et al. showed the sensitivity of the CHP assay demonstrating subfailure micro-damage was detectable in rat tail tendon fascicles under loading, and eventually led to tissue damage observable with other analysis methods [36,43]. Hoy et al. found detected microdamage in the AF in wildtype mouse IVDs with the same dose and duration of AGE organ culture, and used second harmonic generation with multiphoton imaging which is also a very sensitive detection method to detect microdamage [13].

Liu and Tang found decreased proteoglycan and disc height loss in RAGE-KO IVDs compared to wildtype IVDs, and altered biomechanical properties from the same concentration of AGEs in a 21 day organ culture experiment [24], suggesting longer duration would result in more significant damage and degeneration. This 10 day organ culture duration was selected to induce structural and functional changes without concerns over long-term remodeling due to the culture conditions. However, we believe the lack of significant IVD degeneration in this 10 day organ culture study is due to the relatively short duration of these studies, since longer in vivo studies, or more aggressive in vitro challenges in the literature resulted in IVD degeneration and more substantial changes to IVD function [10,12,20,37,48–50]. Sex differences may account for somewhat mild effects observed in this study since this organ culture model used male mice while in vivo studies showed high AGE diet and RAGE-KO had larger effects on female than male spinal tissues [12,49].

AGE challenge to Gal3-KO IVDs resulted in functionally altered biomechanical properties with significantly increased axial compressive stiffness and neutral zone length, and significantly decreased creep elastic displacement and fast time constant. When testing these IVDs biomechanically under force control conditions, collagen damage in the AGE-challenged Gal3-KO IVDs yielded an increased neutral zone, which caused greater compressive stiffness and decreased creep displacement, presumably from IVD tissue compaction or vertebra to vertebra contact. Collagen damage also resulted in decreased fast tissue time constant. Biomechanical damage in this study is consistent with Barbir et al. who measured increased neutral zone and axial compressive stiffness, as well as decreased creep fast time constant in rat IVDs treated with collagenase [51]. The decreased creep elastic displacement in AGE-challenged Gal3-KO IVDs is consistent with reduced creep strain in diabetic rats previously reported [8]. The lack of significant biomechanical alterations from AGE challenge in wildtype and RAGE-KO IVDs further supports the protective role of Gal3 as an AGE receptor in the IVD, and we conclude that AGE challenge resulted in relatively mild damage in wildtype IVDs and more severe damage in Gal3-KO IVDs that were detected on multiple assays.

Gal3 appears to be more important than RAGE in modulating collagen damage and mechanical disruption in the IVD. Numerous studies have found that AGE challenge resulted in collagen damage or altered biomechanical properties both in vivo and in vitro [10,12,13,18,52]. To our knowledge no studies have shown a protective role of Gal3 against AGE challenge in the IVD, though it has been shown in pancreatic islets and adipose tissue [28]. Interestingly, AGE challenge did not cause significantly affected biomechanical changes in wildtype IVDs which did have measurable collagen damage in CHP staining, further supporting the protective role of Gal3. While the protective role of Gal3 as an AGE receptor is a novel finding in the IVD, it is consistent with studies in other organ systems, including in diabetic responses in the liver and kidneys [28,29,31]. AGE-challenged RAGE-KO IVDs did not exhibit significant differences in molecular collagen damage or biomechanical changes, suggesting RAGE plays a role in the damage observed in wildtype and Gal3-KO IVDs. The importance of RAGE in promoting matrix damage and degeneration from AGE exposure, oxidative stress, and diabetes is also supported in the IVD literature [8,13,18,21]. The deleterious role of RAGE in physiological response to AGEs was also found in other organ systems, including the lungs, bone, and the numerous organs influenced by diabetes [53–56]. Together with the literature, results support the hypothesis that Gal3 is protective and RAGE is destructive to IVD tissues and cells in response to AGE challenge.

Gal3 and RAGE appear to interact since AGE challenge decreased Gal3 in wildtype IVDs, and increased RAGE in wildtype and Gal3-KO IVDs. Cross-signaling between Gal3 and RAGE may occur since the well-documented upregulation of RAGE receptor level upon AGE exposure [52,57] was also present for Gal3-KO [21]. The decrease in Gal3 levels in response to AGEs is novel in the IVD, although has been observed in osteoblast and osteosarcoma cell cultures [58]. Gal3 levels were not reduced with AGE exposure for RAGE-KO which may be related to the relatively high variety of possible receptor-ligand interactions for Gal3 so that RAGE-KO does not require a compensatory alteration in Gal3 levels [21]. Furthermore, the decrease in Gal3 levels with AGE challenge may be related to interactions with other matrix glycoproteins in addition to its role as an AGE receptor [21]. The variety of receptor-ligand interactions for Gal3 may therefore suggest Gal3 can offer protective effects in a context-specific manner in the IVD. AGE challenge can therefore affect levels of both RAGE and Gal3 with distinct effects. Previous studies suggest a direct

opposition between RAGE and Gal3 in atherosclerosis and the regulation of vascular osteogenesis with inflammation [59]. Menini et al. also showed that RAGE and Gal3 were involved in Wnt/B-catenin signaling, which has been associated with IVD degeneration through in vitro studies [60–63]. The potential interaction of the AGE receptors in Wnt/B-catenin signaling is especially interesting as Wnt/B-catenin signaling is involved in both the induction of matrix metalloproteinases, which have been implicated in AGE-induced catabolism of the extracellular matrix [18], and in cell proliferation and survival [64–66]. The opposing roles of RAGE and Gal3 in Wnt/B-catenin signaling has been documented in cancer biology research [67,68]. Specifically, RAGE has been shown to diminish cell proliferation and cell survival in osteoblasts by disrupting downstream pro-cell survival targets of Wnt/B-catenin signaling, PI3K and ERK [68]. Conversely, Gal3 has been shown to mediate nuclear B-catenin accumulation by regulating the inhibitory actions of GSK-3B [67,69,70]. Therefore, the current study demonstrates important roles of RAGE and Gal3 as AGE receptors in IVD cells, and the broader literature suggests these receptors may influence Wnt/B-catenin signaling.

Some limitations of this study warrant mention. This mouse organ culture study cannot be directly compared to human dietary patterns, although ~10% of dietary AGEs are absorbed into the circulation, suggesting the AGE-BSA concentration in this study is similar to that expected from a high AGE lab chow [21]. Immunostaining for RAGE and Gal3 positivity did not stain for activated receptors, nevertheless, receptor quantification supports the roles identified in this study with the genetic deletion of Gal3 and RAGE. We focused on AF changes since AF collagen was most susceptible to AGE induced damage which was clearly detected, and NP changes were not apparent from histological measurements. Results demonstrated relatively high biological variability in most parameters, although this variability was controlled using the paired study design in which IVDs from each mouse were treated with control and AGE+ media for each assay and significant results were detected within each genotype. This study was designed to detect effects of AGE+ media treatment within each genotype and therefore applied a paired sample study design to control for biological and technical variance; as a result, the mean differences do not indicate effects as clearly as statistical bars that test pairwise comparisons. Some output measurements had lower sample size because of loss of select samples during staining and processing (even with multiple sections used for each stain), and because of the paired analyses, we needed to exclude both control and AGE+ samples if one of the samples was damaged for that assay. A greater sample size may further allow the detection of effects of genotypes in the control media condition, yet such differences in basal groups can be difficult to interpret since the global deletions are present during development, growth and maturation so that the pairwise analyses were the focus of this study. The presence of notochordal cells may also limit accumulation of some degenerative changes in these mouse IVDs. We therefore note that AGE challenge caused relatively mild effects in our study that were somewhat variable across donors, and we expect more significant changes with greater AGE dose or duration of culture.

We conclude that AGE challenge caused collagen damage in IVDs that was most severe from Gal3-KO mice since differences in CHP and biomechanical properties were detected, less severe in wildtype mice with differences in CHP only, and not detectable in RAGE-KO mice. This AGE challenge directly affected IVD tissues and cells since this organ culture model did not involve systemic in vivo effects. Gal3 therefore appears to play a protective role on IVD cells and tissues in response to an AGE challenge in the IVD, and RAGE was needed for this damage to occur. This study also suggests Gal3 and RAGE interact with downregulation of Gal3 receptor levels and upregulation of RAGE receptor levels upon AGE challenge. We conclude that Gal3 and RAGE are both important receptors in the IVD that differentially control AGE-induced collagen damage, and both need consideration in understanding aging and designing interventions that slow IVD degeneration.

AUTHOR CONTRIBUTIONS

Conception and design of the work: Zachary S. Gallate, Danielle N. D'Erminio, James C. Iatridis. *Acquisition and analysis*: Zachary S. Gallate, Danielle N. D'Erminio, Philip Nasser, Damien M. Laudier. *Interpretation of data for the work*: Zachary S. Gallate, Danielle N. D'Erminio, Philip Nasser, Damien M. Laudier, James C. Iatridis. All authors drafted or critically revised the manuscript for important intellectual content. All authors approved of the final version to be published and agree to be accountable for all aspects of the work in ensuring that questions related to the accuracy or integrity of any part of the work are appropriately investigated and resolved.

ACKNOWLEDGMENTS

Supported by NIH/NIAMS Grants (R01AR069315, R01AR080096, and R01AR078857). Microscopy performed in the Mount Sinai Microscopy CoRE supported by NIH Shared Instrumentation Grant (S10 OD010751).

CONFLICT OF INTEREST STATEMENT

This research was funded by grants from the NIH that were paid to the institution. All authors agree that they have no financial or other agreements that would present a potential conflict of interest with this study. James Iatridis is an Editorial Board member of JOR Spine and a co-author of this article. To minimize bias, they were excluded from all editorial decision-making related to the acceptance of this article for publication. [Correction added on 22 June 2023, after first online publication: Conflict of Interest statement was revised]

ORCID

Zachary S. Gallate https://orcid.org/0000-0001-7512-9122
Danielle N. D'Erminio https://orcid.org/0000-0003-1755-6315
James C. Iatridis https://orcid.org/0000-0002-2186-0590

REFERENCES

1. Dagenais S, Caro J, Haldeman S. A systematic review of low back pain cost of illness studies in the United States and internationally. *Spine J*. 2008;*8*(1):8-20. doi:10.1016/j.spinee.2007.10.005

2. Gore M, Sadosky A, Stacey BR, Tai K-S, Leslie D. The burden of chronic low back pain: clinical comorbidities, treatment patterns, and health care costs in usual care settings. *Spine*. 2012;*37*(11):E668-E677. doi:10.1097/BRS.0b013e318241e5de
3. Fujii K, Yamazaki M, Kang JD, et al. Discogenic back pain: literature review of definition, diagnosis, and treatment. *JBMR Plus*. 2019;*3*(5):e10180. doi:10.1002/jbm4.10180
4. Adams MA, Roughley PJ. What is intervertebral disc degeneration, and what causes it? *Spine*. 2006;*31*(18):2151-2161. doi:10.1097/01.brs.0000231761.73859.2c
5. Iatridis JC, Nicoll SB, Michalek AJ, Walter BA, Gupta MS. Role of biomechanics in intervertebral disc degeneration and regenerative therapies: what needs repairing in the disc and what are promising biomaterials for its repair? *Spine J*. 2013;*13*(3):243-262. doi:10.1016/j.spinee.2012.12.002
6. Vo NV, Hartman RA, Patil PR, et al. Molecular mechanisms of biological aging in intervertebral discs. *J Orthop Res*. 2016;*34*(8):1289-1306. doi:10.1002/jor.23195
7. Eyre DR, Muir H. Types I and II collagens in intervertebral disc. Interchanging radial distributions in annulus fibrosus. *Biochem J*. 1976;*157*(1):267-270. doi:10.1042/bj1570267
8. Fields AJ, Berg-Johansen B, Metz LN, et al. Alterations in intervertebral disc composition, matrix homeostasis and biomechanical behavior in the UCD-T2DM rat model of type 2 diabetes. *J Orthop Res*. 2015;*33*(5):738-746. doi:10.1002/jor.22807
9. Sivan SS, Tsitron E, Wachtel E, et al. Age-related accumulation of pentosidine in aggrecan and collagen from normal and degenerate human intervertebral discs. *Biochem J*. 2006;*399*(1):29-35. doi:10.1042/BJ20060579
10. Wagner DR, Reiser KM, Lotz JC. Glycation increases human annulus fibrosus stiffness in both experimental measurements and theoretical predictions. *J Biomech*. 2006;*39*(6):1021-1029. doi:10.1016/j.jbiomech.2005.02.013
11. Alpantaki K, Kampouroglou A, Koutserimpas C, Effraimidis G, Hadjipavlou A. Diabetes mellitus as a risk factor for intervertebral disc degeneration: a critical review. *Eur Spine J*. 2019;*28*(9):2129-2144. doi:10.1007/s00586-019-06029-7
12. Krishnamoorthy D, Hoy RC, Natelson DM, et al. Dietary advanced glycation end-product consumption leads to mechanical stiffening of murine intervertebral discs. *Dis Model Mech*. 2018;*11*(12):dmm036012. doi:10.1242/dmm.036012
13. Hoy RC, D'Erminio DN, Krishnamoorthy D, et al. Advanced glycation end products cause RAGE-dependent annulus fibrosus collagen disruption and loss identified using in situ second harmonic generation imaging in mice intervertebral disk in vivo and in organ culture models. *JOR Spine*. 2020;*3*(4):e1126. doi:10.1002/jsp2.1126
14. Krishnamoorthy D, D'Erminio DN, Hoy RC, et al. Differing effects of high-fat diet and the receptor for advanced glycation end products on lumbar vertebrae and intervertebral discs In growing male and female mice. *Orthopaedic Research Society Annual Meeting*. Orthopaedic Research Society; 2019. Accessed August 14, 2019. https://www.ors.org/Transactions/65/0169.pdf
15. Hu Y, Shao Z, Cai X, et al. Mitochondrial pathway is involved in advanced glycation end products-induced apoptosis of rabbit annulus fibrosus cells. *Spine*. 2019;*44*(10):E585-E595. doi:10.1097/BRS.0000000000002930
16. Guterl CC, See EY, Blanquer SBG, et al. Challenges and strategies in the repair of ruptured annulus fibrosus. *Eur Cell Mater*. 2013;*25*:1-21. doi:10.22203/eCM.v025a01
17. Illien-Jünger S, Lu Y, Qureshi SA, et al. Chronic ingestion of advanced glycation end products induces degenerative spinal changes and hypertrophy in aging pre-diabetic mice. *PLoS ONE*. 2015;*10*(2):e0116625. doi:10.1371/journal.pone.0116625
18. Illien-Junger S, Grosjean F, Laudier DM, Vlassara H, Striker GE, Iatridis JC. Combined anti-inflammatory and anti-AGE drug treatments have a protective effect on intervertebral discs in mice with diabetes. *PLoS ONE*. 2013;*8*(5):e64302. doi:10.1371/journal.pone.0064302
19. Natelson DM, Lai A, Krishnamoorthy D, Hoy RC, Iatridis JC, Illien-Jünger S. Leptin signaling and the intervertebral disc: sex dependent effects of leptin receptor deficiency and Western diet on the spine in a type 2 diabetes mouse model. *PLoS ONE*. 2020;*15*(5):e0227527. doi:10.1371/journal.pone.0227527
20. Gautieri A, Redaelli A, Buehler MJ, Vesentini S. Age- and diabetes-related nonenzymatic crosslinks in collagen fibrils: candidate amino acids involved in advanced glycation end-products. *Matrix Biol*. 2014;*34*:89-95. doi:10.1016/j.matbio.2013.09.004
21. Ott C, Jacobs K, Haucke E, Navarrete Santos A, Grune T, Simm A. Role of advanced glycation end products in cellular signaling. *Redox Biol*. 2014;*2*:411-429. doi:10.1016/j.redox.2013.12.016
22. Briceno Noriega D, Zenker HE, Croes C-A, et al. Receptor mediated effects of advanced glycation end products (ages) on innate and adaptative immunity: relevance for food allergy. *Nutrients*. 2022;*14*(2):371. doi:10.3390/nu14020371
23. Glaeser JD, Ju D, Tawackoli W, et al. Advanced glycation end product inhibitor pyridoxamine attenuates IVD degeneration in type 2 diabetic rats. *Int J Mol Sci*. 2020;*21*(24):9709. doi:10.3390/ijms21249709
24. Liu J, Tang S. Deletion of RAGE significantly blunts the AGEs- and HMGB1-mediated degeneration of the intervertebral disc. *Trans Orthop Res Soc*. 2018;*43*:749.
25. Vlassara H, Li YM, Imani F, et al. Identification of Galectin-3 As a high-affinity binding protein for advanced glycation end products (AGE): a new member of the AGE-receptor complex. *Mol Med*. 1995;*1*(6):634-646. doi:10.1007/BF03401604
26. Li YM, Mitsuhashi T, Wojciechowicz D, et al. Molecular identity and cellular distribution of advanced glycation endproduct receptors: relationship of p60 to OST-48 and p90 to 80K-H membrane proteins. *Proc Natl Acad Sci U S A*. 1996;*93*(20):11047-11052. doi:10.1073/pnas.93.20.11047
27. Kanai M, Göke M, Tsunekawa S, Podolsky DK. Signal transduction pathway of human fibroblast growth factor receptor 3. Identification of a novel 66-kDa phosphoprotein. *J Biol Chem*. 1997;*272*(10):6621-6628. doi:10.1074/jbc.272.10.6621
28. Pejnovic NN, Pantic JM, Jovanovic IP, et al. Galectin-3 deficiency accelerates high-fat diet-induced obesity and amplifies inflammation in adipose tissue and pancreatic islets. *Diabetes*. 2013;*62*(6):1932-1944. doi:10.2337/db12-0222
29. Pugliese G, Pricci F, Leto G, et al. The diabetic milieu modulates the advanced glycation end product-receptor complex in the mesangium by inducing or upregulating galectin-3 expression. *Diabetes*. 2000;*49*(7):1249-1257. doi:10.2337/diabetes.49.7.1249
30. Hsu DK, Yang RY, Pan Z, et al. Targeted disruption of the galectin-3 gene results in attenuated peritoneal inflammatory responses. *Am J Pathol*. 2000;*156*(3):1073-1083. doi:10.1016/S0002-9440(10)64975-9
31. Iacobini C, Menini S, Oddi G, et al. Galectin-3/AGE-receptor 3 knockout mice show accelerated AGE-induced glomerular injury: evidence for a protective role of galectin-3 as an AGE receptor. *FASEB J*. 2004;*18*(14):1773-1775. doi:10.1096/fj.04-2031fje
32. Menini S, Iacobini C, Blasetti Fantauzzi C, Pesce CM, Pugliese G. Role of Galectin-3 in obesity and impaired glucose homeostasis. *Oxid Med Cell Longev*. 2016;*2016*:9618092. doi:10.1155/2016/9618092
33. Zeng Y, Danielson KG, Albert TJ, Shapiro IM, Risbud MV. HIF-1 alpha is a regulator of galectin-3 expression in the intervertebral disc. *J Bone Miner Res*. 2007;*22*(12):1851-1861. doi:10.1359/jbmr.070620
34. Elshamly M, Kinslechner K, Grohs JG, et al. Galectins-1 and -3 in human intervertebral disc degeneration: non-uniform distribution

profiles and activation of disease markers involving NF-κB by Galectin-1. *J Orthop Res*. 2019;*37*(10):2204-2216. doi:10.1002/jor.24351

35. Tian Y, Yuan W, Li J, et al. TGFβ regulates Galectin-3 expression through canonical Smad3 signaling pathway in nucleus pulposus cells: implications in intervertebral disc degeneration. *Matrix Biol*. 2016;*50*:39-52. doi:10.1016/j.matbio.2015.11.008
36. Zitnay JL, Li Y, Qin Z, et al. Molecular level detection and localization of mechanical damage in collagen enabled by collagen hybridizing peptides. *Nat Commun*. 2017;*8*:14913. doi:10.1038/ncomms14913
37. Rutges JPHJ, Duit RA, Kummer JA, et al. A validated new histological classification for intervertebral disc degeneration. *Osteoarthr Cartil*. 2013;*21*(12):2039-2047. doi:10.1016/j.joca.2013.10.001
38. Laudier D, Schaffler MB, Flatow EL, Wang VM. Novel procedure for high-fidelity tendon histology. *J Orthop Res*. 2007;*25*(3):390-395. doi:10.1002/jor.20304
39. Walter BA, Torre OM, Laudier D, Naidich TP, Hecht AC, Iatridis JC. Form and function of the intervertebral disc in health and disease: a morphological and stain comparison study. *J Anat*. 2015;*227*(6):707-716. doi:10.1111/joa.12258
40. Lai A, Gansau J, Gullbrand SE, et al. Development of a standardized histopathology scoring system for intervertebral disc degeneration in rat models: an initiative of the ORS spine section. *JOR Spine*. 2021;*4*(2):e1150. doi:10.1002/jsp2.1150
41. Walter BA, Korecki CL, Purmessur D, Roughley PJ, Michalek AJ, Iatridis JC. Complex loading affects intervertebral disc mechanics and biology. *Osteoarthritis Cartilage*. 2011;*19*(8):1011-1018. doi:10.1016/j.joca.2011.04.005
42. Hwang J, Huang Y, Burwell TJ, et al. In situ imaging of tissue remodeling with collagen hybridizing peptides. *ACS Nano*. 2017;*11*(10):9825-9835. doi:10.1021/acsnano.7b03150
43. Zitnay JL, Jung GS, Lin AH, et al. Accumulation of collagen molecular unfolding is the mechanism of cyclic fatigue damage and failure in collagenous tissues. *Sci Adv*. 2020;*6*(35):eaba2795. doi:10.1126/sciadv.aba2795
44. Xiao L, Majumdar R, Dai J, et al. Molecular detection and assessment of intervertebral disc degeneration via a collagen hybridizing peptide. *ACS Biomater Sci Eng*. 2019;5(4):1661-1667. doi:10.1021/acsbiomaterials.9b00070
45. Lizotte PP, Hanford LE, Enghild JJ, Nozik-Grayck E, Giles BL, Oury TD. Developmental expression of the receptor for advanced glycation end-products (RAGE) and its response to hyperoxia in the neonatal rat lung. *BMC Dev Biol*. 2007;7:15. doi:10.1186/1471-213X-7-15
46. Mosley GE, Hoy RC, Nasser P, et al. Sex differences in rat intervertebral disc structure and function following annular puncture injury. *Spine*. 2019;*44*(18):1257-1269. doi:10.1097/BRS.0000000000003055
47. O'Connell GD, Jacobs NT, Sen S, Vresilovic EJ, Elliott DM. Axial creep loading and unloaded recovery of the human intervertebral disc and the effect of degeneration. *J Mech Behav Biomed Mater*. 2011;*4*(7):933-942. doi:10.1016/j.jmbbm.2011.02.002
48. Li Y, Fessel G, Georgiadis M, Snedeker JG. Advanced glycation end-products diminish tendon collagen fiber sliding. *Matrix Biol*. 2013;*32*(3–4):169-177. doi:10.1016/j.matbio.2013.01.003
49. D'Erminio DN, Krishnamoorthy D, Lai A, et al. High fat diet causes inferior vertebral structure and function without disc degeneration in RAGE-KO mice. *J Orthop Res*. 2022;*40*(7):1672-1686. doi:10.1002/jor.25191
50. Song Y, Li S, Geng W, et al. Sirtuin 3-dependent mitochondrial redox homeostasis protects against AGEs-induced intervertebral disc degeneration. *Redox Biol*. 2018;*19*:339-353. doi:10.1016/j.redox.2018.09.006
51. Barbir A, Michalek AJ, Abbott RD, Iatridis JC. Effects of enzymatic digestion on compressive properties of rat intervertebral discs. *J Biomech*. 2010;*43*(6):1067-1073. doi:10.1016/j.jbiomech.2009.12.005
52. Song Y, Wang Y, Zhang Y, et al. Advanced glycation end products regulate anabolic and catabolic activities via NLRP3-inflammasome activation in human nucleus pulposus cells. *J Cell Mol Med*. 2017;*21*(7):1373-1387. doi:10.1111/jcmm.13067
53. Sanders KA, Delker DA, Huecksteadt T, et al. RAGE is a critical mediator of pulmonary oxidative stress, alveolar macrophage activation and emphysema in response to cigarette smoke. *Sci Rep*. 2019;*9*(1):231. doi:10.1038/s41598-018-36163-z
54. Yamagishi S. Role of advanced glycation end products (AGEs) in osteoporosis in diabetes. *Curr Drug Targets*. 2011;*12*(14):2096-2102.
55. Goh S-Y, Cooper ME. Clinical review: the role of advanced glycation end products in progression and complications of diabetes. *J Clin Endocrinol Metab*. 2008;*93*(4):1143-1152. doi:10.1210/jc.2007-1817
56. Palimeri S, Palioura E, Diamanti-Kandarakis E. Current perspectives on the health risks associated with the consumption of advanced glycation end products: recommendations for dietary management. *Diabetes Metab Syndr Obes*. 2015;*8*:415-426. doi:10.2147/DMSO.S63089
57. Vlassara H, Striker GE. AGE restriction in diabetes mellitus: a paradigm shift. *Nat Rev Endocrinol*. 2011;*7*(9):526-539. doi:10.1038/nrendo.2011.74
58. Mercer N, Ahmed H, McCarthy AD, Etcheverry SB, Vasta GR, Cortizo AM. AGE-R3/galectin-3 expression in osteoblast-like cells: regulation by AGEs. *Mol Cell Biochem*. 2004;*266*(1–2):17-24. doi:10.1023/b:mcbi.0000049128.71095.ac
59. Menini S, Iacobini C, Ricci C, et al. The galectin-3/RAGE dyad modulates vascular osteogenesis in atherosclerosis. *Cardiovasc Res*. 2013;*100*(3):472-480. doi:10.1093/cvr/cvt206
60. Hiyama A, Sakai D, Risbud MV, et al. Enhancement of intervertebral disc cell senescence by WNT/β-catenin signaling-induced matrix metalloproteinase expression. *Arthritis Rheum*. 2010;*62*(10):3036-3047. doi:10.1002/art.27599
61. Xie H, Jing Y, Xia J, Wang X, You C, Yan J. Aquaporin 3 protects against lumbar intervertebral disc degeneration via the Wnt/β-catenin pathway. *Int J Mol Med*. 2016;*37*(3):859-864. doi:10.3892/ijmm.2016.2470
62. Ye S, Wang J, Yang S, et al. Specific inhibitory protein Dkk-1 blocking Wnt/β-catenin signaling pathway improve protectives effect on the extracellular matrix. *J Huazhong Univ Sci Technol Med Sci*. 2011;*31*(5):657-662. doi:10.1007/s11596-011-0577-y
63. Hiyama A, Yokoyama K, Nukaga T, Sakai D, Mochida J. A complex interaction between Wnt signaling and TNF-α in nucleus pulposus cells. *Arthritis Res Ther*. 2013;*15*(6):R189. doi:10.1186/ar4379
64. Steinhart Z, Angers S. Wnt signaling in development and tissue homeostasis. *Development*. 2018;*145*(11):dev146589. doi:10.1242/dev.146589
65. Logan CY, Nusse R. The Wnt signaling pathway in development and disease. *Annu Rev Cell Dev Biol*. 2004;*20*:781-810. doi:10.1146/annurev.cellbio.20.010403.113126
66. Moon RT. Wnt/beta-catenin pathway. *Sci STKE*. 2005;*2005*(271):cm1. doi:10.1126/stke.2712005cm1
67. Shimura T, Takenaka Y, Fukumori T, et al. Implication of galectin-3 in Wnt signaling. *Cancer Res*. 2005;*65*(9):3535-3537. doi:10.1158/0008-5472.CAN-05-0104
68. Li G, Xu J, Li Z. Receptor for advanced glycation end products inhibits proliferation in osteoblast through suppression of Wnt, PI3K and ERK signaling. *Biochem Biophys Res Commun*. 2012;*423*(4):684-689. doi:10.1016/j.bbrc.2012.06.015

69. Song S, Mazurek N, Liu C, et al. Galectin-3 mediates nuclear beta-catenin accumulation and Wnt signaling in human colon cancer cells by regulation of glycogen synthase kinase-3beta activity. *Cancer Res*. 2009;*69*(4):1343-1349. doi:10.1158/0008-5472.CAN-08-4153
70. Kim S-J, Choi I-J, Cheong T-C, et al. Galectin-3 increases gastric cancer cell motility by up-regulating fascin-1 expression. *Gastroenterology*. 2010;*138*(3):1035-45.e1. doi:10.1053/j.gastro.2009.09.061

SUPPORTING INFORMATION

Additional supporting information can be found online in the Supporting Information section at the end of this article.

How to cite this article: Gallate, Z. S., D'Erminio, D. N., Nasser, P., Laudier, D. M., & Iatridis, J. C. (2023). Galectin-3 and RAGE differentially control advanced glycation endproduct-induced collagen damage in murine intervertebral disc organ culture. *JOR Spine*, *6*(2), e1254. https://doi.org/10.1002/jsp2.1254